Synergistic removal of copper and tetracycline from aqueous solution by steam-activated bamboo-derived biochar

Rong-Zhong Wang[a,b], Dan-Lian Huang[a,b,*], Yun-Guo Liu[a,b], Chen Zhang[a,b], Cui Lai[a,b], Xin Wang[c], Guang-Ming Zeng[a,b], Qing Zhang[a,b], Xiao-Min Gong[a,b], Piao Xu[a,b]

[a] College of Environmental Science and Engineering, Hunan University, Changsha, 410082, People's Republic of China
[b] Key Laboratory of Environmental Biology and Pollution Control (Hunan University), Ministry of Education, Changsha, 410082, People's Republic of China
[c] School of Materials Science and Engineering, Xi'an Jiaotong University, Xi'an, 710049, People's Republic of China

GRAPHICAL ABSTRACT
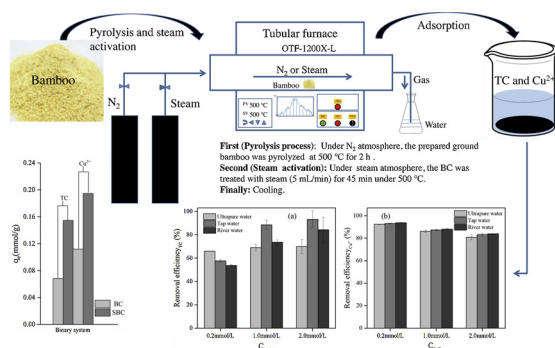
ARTICLE INFO

ABSTRACT

Steam-activated biochar (SBC) was prepared and showed excellent performance for synergistic removal of Cu^{2+} and tetracycline (TC). The adsorption capacity of SBC and mutual effect of TC and Cu^{2+} were investigated via single and binary system and the adsorption isotherm. The adsorption capacity of TC was significantly enhanced when it coexisted with Cu^{2+}. Likewise, increased amounts of Cu^{2+} were adsorbed in the presence of TC. The presence of NaCl exerted a negative influence on the adsorption of Cu^{2+}, while the inhibitory effect of salinity on TC was neutralized by bridge enhancement in the binary system. Bridge enhancement and site competition were involved in the synergistic removal of TC and Cu^{2+}. Considering the stable application in simulated and real water samples, SBC showed great potential for synergistic removal of antibiotics and heavy metals.

1. Introduction

Environmental pollution has become increasingly serious (Qasemi et al., 2018a, 2019; Qasemi et al., 2018b; Rezaei et al., 2019); in particular, the combined pollution of heavy metals and antibiotics has gained wide public attention (Chen et al., 2016; Gong et al., 2017; Ling et al., 2013). Cu^{2+} has been extensively used as a feed additive in the livestock and poultry industry because of its growth-promoting effect. However, Cu^{2+} cannot be degraded and is released into the environment (Ding et al., 2018). Meanwhile, tetracycline (TC), which is a typical antibiotic (Dehghan et al., 2018), has been widely used in livestock breeding (Sarmah et al., 2006). Owing to the poor metabolization

---

or absorption of TC in *vivo*, 40–90% of parent compounds are discharged into aquatic environments (Sarmah et al., 2006). Therefore, the surrounding water body is easily polluted by TC and Cu^{2+} simultaneously. TC and Cu^{2+} are harmful to animals and humans. Moreover, TC and Cu^{2+} can easily form complexes, which make their environmental behaviors more complicated. The toxicity of complex species is generally greater than that of precursors (Ling et al., 2013). Therefore, it is imperative to remediate combined pollution.

Various methods have been used to remove antibiotics and heavy metals, including ion exchange, chemical precipitation, membranes, adsorption, etc. (Guo et al., 2018; Huang et al., 2016; Zhou et al., 2017a; Dehghani et al., 2018; Qasemi et al., 2018c). Owing to its advantages, including its low cost, high efficiency (Gong et al., 2018; Dehghani et al., 2017a,b), simplicity of design (Huang et al., 2015; Fazlzadeh et al., 2017a; Khosravi et al., 2018a), and ease of operation (Zhou et al., 2018; Fazlzadeh et al., 2017b), adsorption among the most reliable alternatives. However, it is more difficult to simultaneously remove antibiotics and heavy metals than it is to remove single pollutants because of (i) competition for the adsorption site, (ii) strong complexation of solutes, or (iii) formation of ternary surface complexes (Ling et al., 2013). Thus, selection of the adsorbent is very important.

Biochar (BC) is an emerging carbon-rich material produced by biomass pyrolysis under no or oxygen-limited conditions (Huang et al., 2019a, 2018; Gong et al., 2019). It possesses a porous structure, abundant surface functional groups, and high specific surface area, which are conducive to the removal of heavy metals and antibiotics (Huang et al., 2019b). In addition, BC can be produced from a variety of raw materials such as agricultural residues, sewage sludge, and livestock manure. BC may be an appropriate alternative to remove pollutants. Recently, steam-activated biochar (SBC) has displayed good adsorption capacity for separate organic pollutants or heavy metals (Rajapaksha et al., 2015; Shim et al., 2015). It is possible to enhance the pore volume and surface area of BC by removing the trapped products of incomplete combustion during thermal treatment and can then enhance the adsorption capacity of pollutants (Rajapaksha et al., 2014). Furthermore, it is relatively simple and economically feasible (Rajapaksha et al., 2016). SBC may have the potential to simultaneously remove antibiotics and heavy metals. Antibiotics can form complexes with heavy metals, which may influence the removal efficiency of pollutants. It is necessary to study the mutual effect of coexistent pollutants. Additionally, the removal mechanisms of Cu^{2+} and TC in binary systems are much more complicated than those in single systems. Thus, the mechanisms of simultaneously removing TC and Cu^{2+} by SBC need to be studied.

Thus, a bamboo-SBC was synthesized for the removal of Cu^{2+} and TC, and the main experimental contents of this research included (i) discussion of the mutual effect of coexisting pollutants on the removal of TC or Cu^{2+}; (ii) study of the simultaneous adsorption ability of SBC for TC and Cu^{2+} using key parameters (the initial concentration of TC or Cu^{2+}, pH, and ionic strength) and applications in tap water and Xiangjiang River water; and (iii) investigation of underlying mechanisms of TC and Cu^{2+} adsorption onto SBC.

2. Materials and methods

2.1. Materials

All chemicals, including HCl, NaOH, NaCl, Na_2CO_3, $MnCl_2 \cdot 4H_2O$, KH_2PO_4, $MgCl_2 \cdot 6H_2O$, $CaCl_2 \cdot 6H_2O$, $Pb(NO_3)_2$, and $Cu(NO_3)_2 \cdot 3H_2O$, were analytical reagent grade. All solutions were prepared using ultrapure water (resistivity of 18.25 MΩ/cm). TC (purity of 99.5%) was purchased from the Sigma-Aldrich Chemical Co.

2.2. Preparation of steam-activated biochar

The bamboo was obtained from local farmers (28°18'N, 112°41'E),

and was washed several times. It was subsequently dried at 60 °C and smashed to pass through a 100 mesh sieve (0.147 mm). Under oxygen-limited conditions, the prepared ground bamboo was pyrolyzed in an OTF-1200X-L tubular furnace with a heating rate of approximately 8 °C /min. The bamboo was pyrolyzed at 500 °C for 2 h. After, the BC was treated with steam (5 mL/min) for 45 min under 500 °C (Rajapaksha et al., 2015). The samples obtained from bamboo with and without steam activation were called SBC and BC, respectively.

2.3. Batch adsorption experiment

To investigate the adsorption behavior of TC and Cu^{2+} on SBC, batch adsorption experiments were conducted. The adsorption experiments were conducted in three different modes, namely (i) Mode 1: Cu^{2+} only, (ii) Mode 2: TC only, and (iii) Mode 3: Cu^{2+} and TC mixture. First, 0.02 g of BC was added to a 20 mL solution in vials. Then, 0.1 M HNO_3 and NaOH solution was applied to regulate the desired pH. The adsorption capacities of SBC and BC were compared with the initial Cu^{2+} concentration in the range of 0–3 mmol/L and initial TC concentration in the range of 0–0.6 mmol/L. The effect of pH on the adsorption of Cu^{2+} and TC by SBC was determined with an initial pH range from 2 to 7. The effect of ionic strength on the removal of TC and Cu^{2+} by SBC was investigated with an NaCl concentration range of 0 mmol/L to 100 mmol/L. The effects of $CaCl_2$, $MgCl_2$, $MnCl_2$, $Pb(NO_3)_2$, Na_2CO_3, and KH_2PO_4 on the adsorption of TC and Cu^{2+} were also studied. The concentration of each of the six electrolytes was 100 mmol/L. After the adsorption experiment, the mixtures were collected and filtered through 0.45 μm pore size nylon filters. The residual concentrations of Cu^{2+} and TC were determined.

2.4. Measurement of the Cu^{2+} and tetracycline concentrations

Atomic adsorption spectrophotometry (THERMO, USA) and UV–vis spectrometry (Agilent 8453, USA) were applied to detect the residual concentrations of Cu^{2+} and TC, respectively. According to the following Eqs. (1) and (2), the removal efficiency and adsorption capacity (q; mg/g) of Cu^{2+} or TC on SBC were calculated. The limit of detection (LOD) and limit of quantification (LOQ) of the method for Cu^{2+} were 0.008 mg/L and 0.032 mg/L, respectively. The LOD and LOQ of the method for TC was 0.017 mg/L and 0.068 mg/L, respectively. Furthermore, the value of q_{TC}/q_{Cu} was the ratio of the adsorption capacity of TC to the adsorption capacity of Cu^{2+}. Meanwhile, the value of q_{Cu}^{2+}/q_{TC} was the ratio of the adsorption capacity of Cu^{2+} to the adsorption capacity of TC.

$$Adsorption \ (A) \ \% = (C_0 - C_e)/C_0 \qquad (1)$$

$$q = (C_0 - C_e) * V/m \qquad (2)$$

where C_0 and C_e are the initial and equilibrium concentrations of Cu^{2+} or TC (mg/L), respectively; V is the volume of the solution (L); and m is the weight of added SBC (g).

2.5. Characterization methods

Many characterization methods were applied to investigate the physicochemical properties of SBC, and the detailed methods are described in our previous study (Wang et al., 2018). To study the underlying mechanisms of TC and Cu^{2+} adsorption onto SBC, X-ray photoelectron spectroscopy (XPS) was applied to study the changes in surface functional groups in SBC before and after adsorption in single and binary systems.

Table 1
Physicochemical properties of BC and SBC.

	BC	SBC
pH	10.02	10.86
Ash (%)	4.57	5.05
C (%)	81.53	82.52
H (%)	4.45	4.39
O (%)	13.14	10.80
N (%)	0.11	0.18
Molar H/C ($\times 10^{-1}$)	0.55	0.53
Molar O/C	0.16	0.13
Molar (O + N)/C	0.16	0.13
Surface area ($m^2 g^{-1}$)	1.22	2.12
Pore volume ($\times 10^{-1} cm^3 g^{-1}$)	0.01	0.02
Pore diameter (nm)	1.85	4.06

3. Results and discussion

3.1. Properties of the prepared biochar material

After steam activation, the characteristics of BC may change. Table 1 presents the physicochemical characteristics of BC and SBC. Compared with BC, SBC had a higher ash content and pH. Similar results were observed by Rajapaksha (Rajapaksha et al., 2015). The total C content was slightly increased after steam activation. Generally, the H/C and (O + N)/C ratios are used to predict the aromaticity and polarity of BC, respectively. It was observed that the H/C ratio of SBC did not change much. Meanwhile, the polarity index ((O + N)/C) of SBC was lower than that of BC, thereby suggesting that the surface polar functional groups concentration decreased (Rajapaksha et al., 2014). In addition, the reduction of the molar O/C ratio may have reduced the hydrophilic properties of BC (Shim et al., 2015). The specific surface area and pore volume of the SBC were slightly larger than those of the BC. Azargohar and Dalai (2008) also found that steam activation can increase the total pore volume of BC samples, which favors the adsorption of pollutants.

The C1s spectrum of BC was deconvoluted into four peaks at 284.6, 285.2, 287.3 and 289.7 eV, which were associated with C, C−O, C=O and O−C=O, respectively (Fig. 1). After steam activation, the ratio of graphitic carbon increased, which was advantageous to the removal of TC. The graphite-like structure could act as a π-acceptor and interact with the protonated aniline ring of the TC molecule. The ratios of C−O and C=O both decreased. Conversely, the ratio of O−C=O increased from 9.65% to 17.97% after steam activation, which was consistent with the results of Mandal et al. (2017). The O−C=O group was beneficial for the adsorption of heavy metals and organic pollutants. These findings suggested that steam activation influenced the properties of BC and that some effects were beneficial for the removal of pollutants.
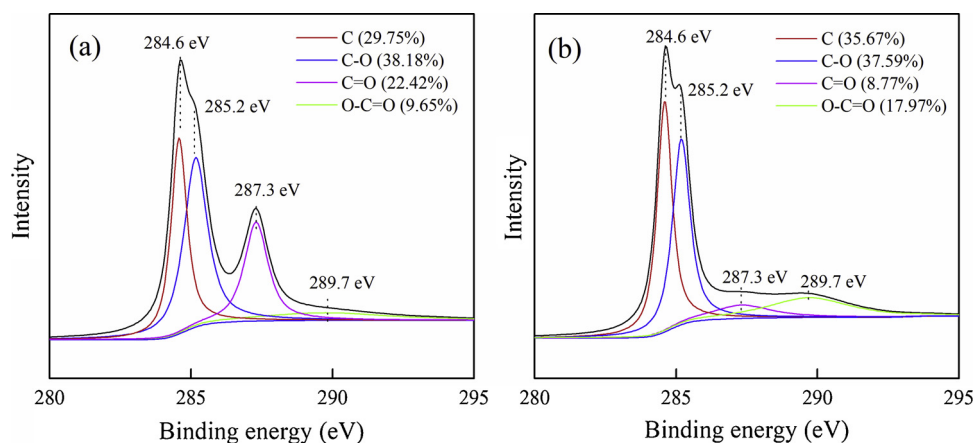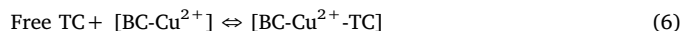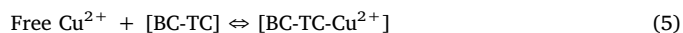
3.2. Mutual effect of Cu^{2+} and tetracycline uptake by steam-activated biochar and biochar

Studies have shown that the mutual effect of Cu^{2+} and TC uptake is complicated. On one hand, Cu^{2+} and TC can easily form complexes. This may be beneficial for the synergistic removal of Cu^{2+} and TC. The complexes are predominately in the form of [Cu-TC], [Cu-TC]$^+$, [CuTC]^0 with a minor quantity of the [Cu-2TC] complex (Ling et al., 2013). In addition, the promotive effect of complexes can be described by Eqs. (3)–(6). On the other hand, Cu^{2+} and TC may be absorbed by the same adsorption sites and compete for the adsorption sites (Chen et al., 2016). Thus, the mutual effects of Cu^{2+} and TC uptake by SBC and BC were investigated.

$$Free\ Cu^{2+} + BC \Leftrightarrow [BC\text{-}Cu^{2+}] \tag{3}$$

$$Free\ TC + BC \Leftrightarrow [BC\text{-}TC] \tag{4}$$

$$Free\ Cu^{2+} + [BC\text{-}TC] \Leftrightarrow [BC\text{-}TC\text{-}Cu^{2+}] \tag{5}$$

$$Free\ TC + [BC\text{-}Cu^{2+}] \Leftrightarrow [BC\text{-}Cu^{2+}\text{-}TC] \tag{6}$$

3.2.1. Impact of the initial tetracycline concentration on the adsorption of Cu^{2+}

The impact of the initial TC concentration on the removal of Cu^{2+} by SBC and BC was investigated with the increase in initial TC concentration from 0 mmol/L to 0.6 mmol/L. As shown in Fig. 2a, the adsorption of Cu^{2+} increased in the presence of TC. When the initial concentration of TC ranged from 0.05 mmol/L to 0.40 mmol/L, the adsorption capacity of Cu^{2+} gradually increased. Meanwhile, the adsorption of TC by SBC increased (Fig. 2b). The increased amount of Cu^{2+} may have been adsorbed owing to the complexation with the increased in adsorbed TC molecules (Eq. (5)), and the complex may have acted as a bridge between Cu^{2+} and the adsorbent (Ma et al., 2014). However, when the initial TC concentration increased to 0.6 mmol/L, the adsorption of Cu^{2+} decreased. A large amount of TC may have occupied the adsorption sites and competed with Cu^{2+}, thereby leading to the decrease in Cu^{2+} adsorption (Ma et al., 2014). Similarly, the uptake of Cu^{2+} by BC was also enhanced when TC co-existed in the solution. Most importantly, when the initial TC concentration ranged from 0 mmol/L to 0.6 mmol/L, the adsorption capacity of SBC was higher than that of BC.

In addition, in order to understand the adsorption process of TC and Cu^{2+} by SBC in binary systems, the q_{Cu}/q_{TC} values are evaluated and the obtained results are shown in Fig. 2c. When the concentration of TC was 0.05 mmol/L, the value of q_{Cu}/q_{TC} was larger than 3. This could be explained by the fact that the concentration of Cu^{2+} (0.20 mmol/L) was larger than that of TC (0.05 mmol/L), and most of the Cu^{2+} was
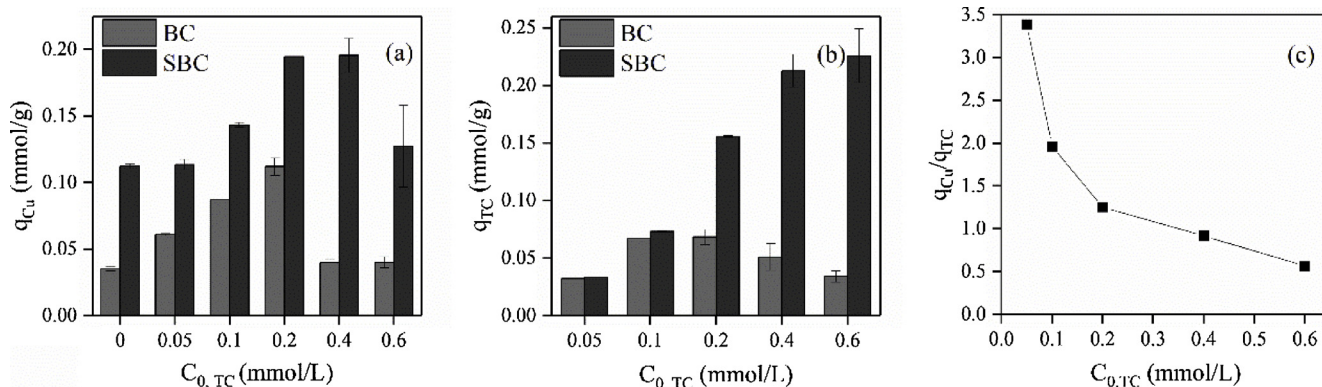

Fig. 1. X-ray photoelectron spectroscopy spectra of biochar (BC) (a) and steam-activated biochar (SBC) (b).

Fig. 2. Effect of the concentration of tetracycline (TC) on the adsorption of Cu^{2+} (a) and TC (b), and the ratio of q_{Cu}/q_{TC} (c) by biochar (BC) and steam-activated biochar (SBC) (dosage = 1.0 g/L; $C_{0,\ Cu^{2+}}$ was fixed at 0.2 mmol/L; $C_{0,\ TC}$ ranged from 0–0.6 mmol/L; 298 K; pH = 5).

removed by way of Eq. (3) instead of Eq. (5). When the concentration of TC increased to 0.2 mmol/L and the concentration of Cu^{2+} was 0.2 mmol/L, the value of q_{Cu}/q_{TC} was larger than 1, thereby suggesting that the adsorption capacity of SBC for Cu^{2+} was higher than that for TC. When the concentration of TC increased to 0.6 mmol/L, the value of q_{Cu}/q_{TC} was reduced to less than 1. The initial concentration of Cu^{2+} (0.2 mmol/L) was significantly lower than that of TC (0.6 mmol/L), a large amount of TC was adsorbed, and a relatively small amount of Cu^{2+} was removed. These results were consistent with those obtained by Ma et al. (2014). In conclusion, when the initial concentration of TC increased from 0.05 mmol/L to 0.40 mmol/L, the adsorption of Cu^{2+} (0.20 mmol/L) by SBC gradually increased. Once the concentration of TC exceeded 0.4 mmol/L, the bridge enhancement decreased and the competition effect was enhanced, so the adsorption capacity and enhancement were decreased.

3.2.2. Effect of the initial Cu^{2+} concentration on the adsorption of tetracycline

The effect of the initial Cu^{2+} concentration on the removal of TC by SBC and BC is shown in Fig. 3. With the addition of Cu^{2+}, the adsorption capacity of TC significantly increased. When the initial concentration of Cu^{2+} increased from 0.2 mmol/L to 1.0 mmol/L, the adsorption capacity of TC by SBC gradually increased (Fig. 3a). Meanwhile, the adsorption of Cu^{2+} also increased (Fig. 3b). It was suggested that the complexation-bridging between Cu^{2+} and TC on the adsorbent increased the adsorption amount of TC (Ling et al., 2013). However, when the concentration of Cu^{2+} continued to increase, the adsorption amount of TC decreased (Fig. 3a). This phenomenon may have been attributed to the fact that Cu^{2+} occupied more active sites than TC, thereby leading to the decrease in TC adsorption. Chen et al.

also found similar results (Chen et al., 2016). In brief, when the initial concentration of Cu^{2+} increased from 0.2 mmol/L to 1.0 mmol/L, the adsorption of TC (0.2 mmol/L) by SBC gradually increased. Once the concentration of Cu^{2+} increased to more than 1.0 mmol/L, the competition effect increased and neutralized part of the bridge enhancement. The adsorption capacity and enhancement were decreased. In addition, when the initial Cu^{2+} concentration was in the range of 0–3.0 mmol/L, the adsorption capacity of SBC for Cu^{2+} was higher than that of BC, thereby suggesting that steam activation was conducive to increasing the adsorption capacity of BC.

As shown in Fig. 3c, when the initial concentration of Cu^{2+} increased from 0.2 to 3.0 mmol/L, the ratio of q_{TC}/q_{Cu} decreased. Cu^{2+} ions were compactly distributed on the SBC surface and was accompanied by more significant steric resistance (Ma et al., 2014), thereby leading to the decreased adsorption of TC. In addition, the values of q_{TC}/q_{Cu} were lower than 1, thereby indicating that a small amount of the adsorbed Cu^{2+} ions was attached to TC.

3.3. Adsorption isotherm

The Langmuir isotherm assumes that the surface of the adsorbent is uniform and that no interactions between adsorbate molecules on adjacent sites exist. The Freundlich isotherm deems that multilayer adsorption is involved in the uptake of pollutants (Zhou et al., 2017b; Naghizadeh et al., 2016). The equations are expressed as follows (Qasemi et al., 2018d):

$$Q_e = K_L Q_m C_e / (1 + K_L C_e) \tag{7}$$
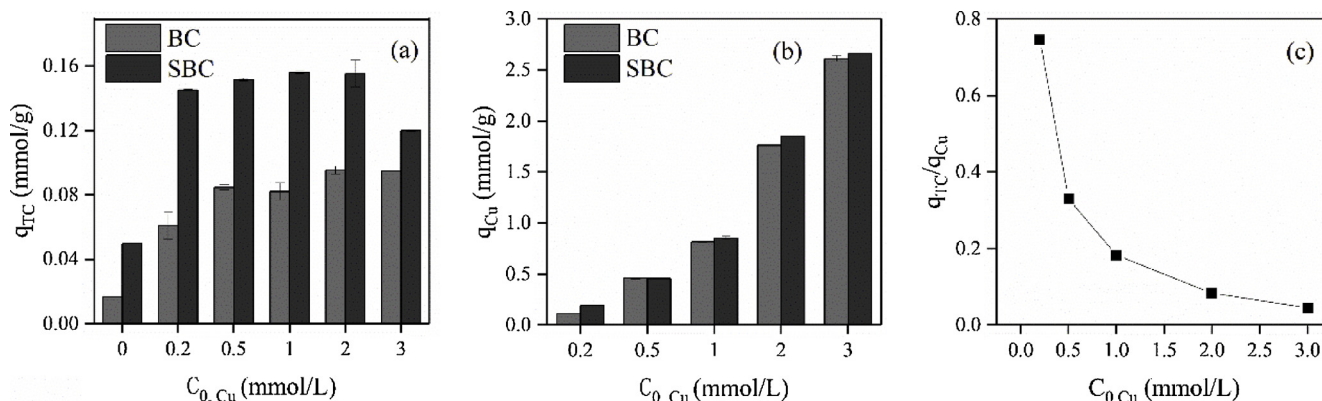
$$Q_e = K_F C_e^{1/n} \tag{8}$$

Fig. 3. Effect of the concentration of Cu^{2+} on the adsorption of tetracycline (TC) (a) and Cu^{2+} (b), and the ratio of q_{TC}/q_{Cu} (c) by biochar (BC) and steam-activated biochar (SBC) (dosage = 1.0 g/L; $C_{0,\ TC}$ was fixed at 0.2 mmol/L; $C_{0,\ Cu^{2+}}$ ranged from 0 to 3 mmol/ L; 298 K; pH = 5).
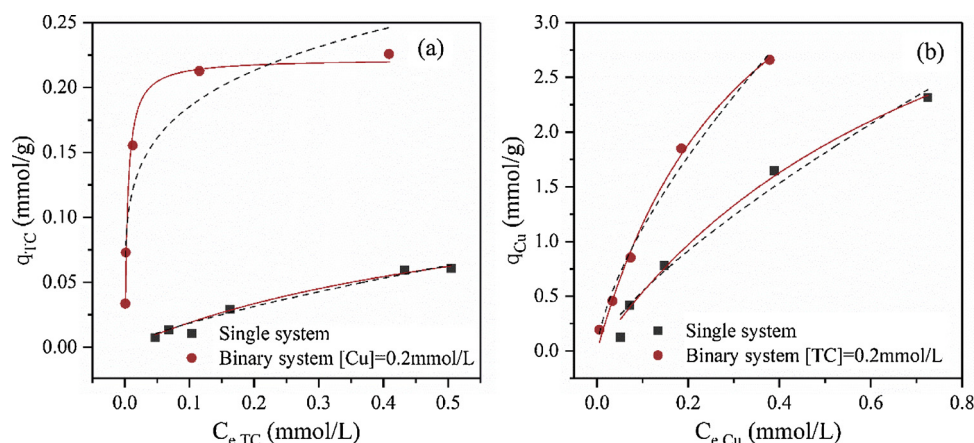
Fig. 4. Adsorption isotherms of tetracycline (TC) (a) and Cu^{2+} (b) in single and binary systems fitted by the Langmuir model (solid lines) and Freundlich model (dashed lines) (dosage = 1.0 g/L; $C_{0, TC}$ ranged from 0–0.6 mmol/L; $C_{0, Cu^{2+}}$ ranged from 0 to 3 mmol/ L, respectively; 298 K; pH = 5).

where Q_m (mg/g) is the maximum adsorption capacity; Q_e (mg/g) and C_e (mg /L) are the amount of adsorbed Cu^{2+} or TC and the concentration of Cu^{2+} or TC in the solution at equilibrium, respectively; K_L is the affinity constant; and K_F (mg g^{-1}) and n are the adsorption equilibrium constant.

The adsorption isotherms of Cu^{2+} and TC onto SBC were determined in single and binary systems. The Langmuir and Freundlich models were used to simulate the experimental process. As displayed in Fig. 4 and Table 2, it was found that the Langmuir equation could better describe the sorption isotherm of Cu^{2+} and TC, thereby suggesting that homogeneous adsorption of TC and Cu^{2+} occurred on the adsorbent and the adsorption of SBC was likely monolayer (Wang et al., 2018). The K_L and q_{max} values in the binary system were higher than those in the single system. Furthermore, compared with other materials, the prepared SBC showed better adsorption performance for TC and Cu^{2+} (Table 3). SBC was a good alternative for simultaneously removing TC and Cu^{2+}.

3.4. Influence of pH on tetracycline and Cu^{2+} removal

pH is a key parameter in the adsorption of heavy metals or antibiotics because it may affect the surface charge of the material and the speciation of TC (Huang et al., 2017; Lai et al., 2016). Thus, the influence of solution pH on the removal of TC and Cu^{2+} was studied. As presented in Fig. 5 a, the adsorption capacities of Cu^{2+} in the single and binary systems increased with the increase in pH. This phenomenon was mainly ascribed to the Zeta potential of SBC. The point of zero charge (pH_{pzc}) of SBC was 2–3. When pH < pH_{pzc}, the hydroxyl and carboxylic groups of SBC were protonated, and the surface of SBC was positively charged. Electrostatic repulsion between SBC and Cu^{2+} decreased the adsorption capacity. When pH > pH_{pzc}, the hydroxyl and carboxylic groups of SBC were deprotonated (Zhou et al., 2016), and $[Cu-TC]^+$ and Cu^{2+} were existed in solution (Ling et al., 2013), so the electrostatic attraction between SBC and the pollutant increased,

thereby increasing the adsorption capacity (Yap et al., 2016).

Different from the uptake of Cu^{2+}, when the pH ranged from 2 to 7, the adsorption capacity of TC in the single and binary system increased and then decreased (Fig. 5 b). As the pH increased from 2 to 5, the adsorption amount of TC gradually increased. However, as the pH further increased, the adsorption capacity of TC decreased. These results could have been attributed to the Zeta potential of SBC and the pH-dependent speciation of TC. At a pH of 2, TC mainly existed in cationic form (TC^+ or H_3TC^+) (Ling et al., 2013) and the hydroxyl and carboxylic groups of SBC were protonated, so the electrostatic repulsion caused low adsorption (Zhao et al., 2013). When the pH ranged from 3 to 5, the hydroxyl and carboxylic groups of SBC were deprotonated, so the electrostatic interaction between H_3TC^+ and negatively charged SBC surfaces increased the uptake of TC in the single system (Rajapaksha et al., 2014; Zhao et al., 2013). In the binary system, the percentage of TC^+ decreased while the percentage of $[Cu-TC]^+$ significantly increased. $[Cu-TC]^+$ became the dominant species in the binary system. The electrostatic interaction between $[Cu-TC]^+$ or TC^+ and negatively charged SBC surfaces increased the uptake of TC (Ling et al., 2013). When the pH value ranged from 5 to 7, the percentage of H_3TC^+ or $[Cu-TC]^+$ decreased, and the percentage of HTC^- or $[Cu-TC]^0$ gradually increased (Ling et al., 2013; Zhao et al., 2013), so the electrostatic interaction between TC and SBC decreased, thereby causing the decrease in TC adsorption. Moreover, as illustrated in Fig. 5(b), Cu^{2+} did not alter the tendency of TC adsorption in solutions with different pH, but significantly enhanced the adsorption amount of TC.

3.5. Influence of ionic strength on tetracycline and Cu^{2+} removal

Ions universally exist in the environment, including in natural water and wastewater streams, and they may affect the adsorption capacity of TC and Cu^{2+} (Wang et al., 2018). Thus, the influences of coexisting ions on the removal of TC and Cu^{2+} were investigated, and the results are illustrated in Fig. 6. With the addition of NaCl, the adsorption capacities of Cu^{2+} in the single and binary systems slightly decreased (Fig. 6a). This could be explained as follows: (i) Cu^{2+} and Na^+ can compete for the same adsorption sites (Wang et al., 2015); (ii) the addition of Na^+ can suppress the electrostatic interactions between the adsorbent and adsorbate by the electrostatic screening effect (Jung et al., 2018); and (iii) anions (Cl^-) also compete with Cu^{2+} for the active site through the mechanisms of charge diffusion and competitive adsorption (Baig et al., 2014; Hong et al., 2017). Compared with NaCl, other coexisting ions ($CaCl_2$, $MgCl_2$, $MnCl_2$, $Pb(NO_3)_2$, Na_2CO_3 and KH_2PO_4) had greater impacts on the adsorption of Cu^{2+} (Fig. 6(c)). These coexisting cations may have had a much greater screening effect on the electrostatic

Table 2
The isotherm parameters for TC and Cu^{2+} adsorption onto SBC.

Target	Langmuir model			Freundlich model		
	K_L	q_m (mmol/g)	R_{adj}^2	K_F	1/n	R_{adj}^2
TC	1.5180	0.144	0.9950	0.1067	0.7580	0.9882
TC in binary solution	235.643	0.222	0.9920	0.2950	0.2015	0.8795
Cu^{2+}	1.2068	5.010	0.9903	3.0358	0.7437	0.9779
Cu^{2+} in binary solution	3.0063	5.029	0.9952	5.1933	0.6651	0.9899

Table 3
The comparison of remove efficiencies for TC and Cu^{2+} by SBC and other materials.

Target	Concentration (mmol/L)	Conditions (mmol/L)	q_{max} (mmol/g)	Material	Ref.
TC	0~0.6	[Cu] = 0	0.011	Chelating Resin	(Ling et al., 2013)
		[Cu] = 0.2	0.029		
TC	0~0.25	[Cu] = 0	0.054	Amino-Fe(III) functionalized mesoporous silica	(Zhang et al., 2015)
		[Cu] = 0.25	0.093		
TC	0~0.2	[Cu] = 0	0.039	Zeolite	(Huang et al., 2012)
		[Cu] = 0.1	0.154		
TC	0~1.06	[Cu] = 0	0.054	Chitosan	(Jin et al., 2010)
		[Cu] = 0.25	0.087		
		[Cu] = 0.50	0.093		
TC	0~0.5	[Cu] = 0	0.066	Struvite-loaded zeolite	(Wang et al., 2019)
TC	0~0.6	[Cu] = 0	0.144	SBC	This study
		[Cu] = 0.2	0.222		
Cu^{2+}	0~3.0	[TC] = 0	1.208	Chelating Resin	(Ling et al., 2013)
		[TC] = 0.2	1.418		
Cu^{2+}	0~2.5	[TC] = 0	0.475	Amino-Fe(III) functionalized mesoporous silica	(Zhang et al., 2015)
		[TC] = 0.1	0.567		
Cu^{2+}	0~2.0	[TC] = 0	1.856	Chitosan	(Jin et al., 2010)
		[TC] = 0.1	1.486		
Cu^{2+}	0~0.6	[TC] = 0	2.182	Struvite-loaded zeolite	(Wang et al., 2019)
		[TC] = 0.1	0.379		
		[TC] = 0.35	0.166		
Cu^{2+}	0~3.0	[TC] = 0	5.010	SBC	This study
		[TC] = 0.2	5.029		

interaction between Cu^{2+} and SBC than that of NaCl. In addition, these coexisting cations occupied more active adsorption sites, which were available for Cu^{2+} bonding.

The impact of ionic strength on the adsorption of TC was different from that of Cu^{2+}. As illustrated in Fig. 6b, when the concentration of NaCl increased, the adsorption capacity of TC increased and then decreased in the single system. This phenomenon may have been attributed to the synergistic effect of the promotive salting-out effect and the inhibitive electrostatic screening effect of Na^+ (Ma et al., 2014; Yu et al., 2017). In addition, Cl^- also had a negative effect on the adsorption of TC. The interaction between anions (Cl^-) and the negatively charged SBC surface made it strongly repellent and have a weak affinity for TC (Zeng et al., 2017). Different from the impact of ionic strength in the single system, the adsorption of TC in the binary system was not inhibited by the presence of NaCl, and the adsorption amount of TC in the binary system was higher than that of the single system. Cu^{2+} formed a bridge between the SBC and TC and increased the adsorption capacity, which neutralized the inhibitive effect of NaCl. However, the adsorption of TC in the binary system was inhibited by the presence of $CaCl_2$, $MgCl_2$, $MnCl_2$, $Pb(NO_3)_2$, Na_2CO_3, and KH_2PO_4. The adsorption capacities of TC in the presence of coexisting cations were in the order of NaCl > $Pb(NO_3)_2$ > $CaCl_2$ > $MnCl_2$ > $MgCl_2$ > Na_2CO_3 > KH_2PO_4.

These coexisting cations occupied more active adsorption sites for TC than NaCl. In addition, the bridge enhancement of Cu^{2+} could not neutralize the inhibitive effect of these coexisting cations.

3.6. Thermodynamic study

Thermodynamic studies were conducted to evaluate whether the adsorption process was spontaneous. Three basic thermodynamic parameters, namely standard Gibbs free energy (ΔG^0; kJ/mol)), standard enthalpy change (ΔH^0; kJ/mol)), and standard entropy change (ΔS^0; J/mol·K), were calculated according to the following equation (Khosravi et al., 2018b):

$$\Delta G^0 = -RT \ln K^0 \tag{9}$$

where K^0 is a thermodynamic equilibrium constant. It was calculated by plotting $\ln(Q_e/C_e)$ as a function of Q_e. Q_e (mg/g) and C_e (mg/L) are the amount of adsorbed Cu^{2+} or TC and the Cu^{2+} or TC concentration in the solution at equilibrium, respectively. R is the universal gas constant (8.3145 J/(mol·K)) and T is the temperature of the solution (K). ΔH^0 (kJ/mol) and ΔS^0 (J/(mol·K)) could be calculated using the van't Hoff equation, as follows:
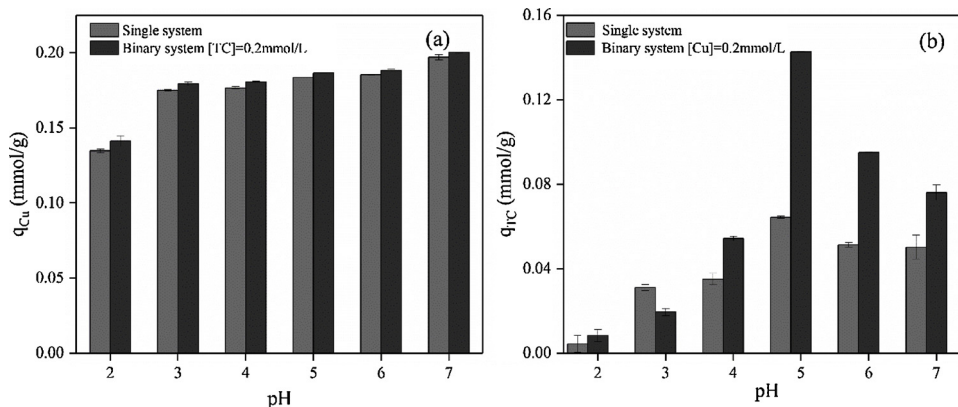

Fig. 5. Effect of pH on the adsorption of Cu^{2+} (a) and tetracycline (TC) (b) in the single and binary systems (dosage = 1.0 g/L; $C_{0, Cu^{2+}}$ was fixed at 0.2 mmol/L (a); $C_{0, TC}$ was 0.15 mmol/L (b); 298 K).
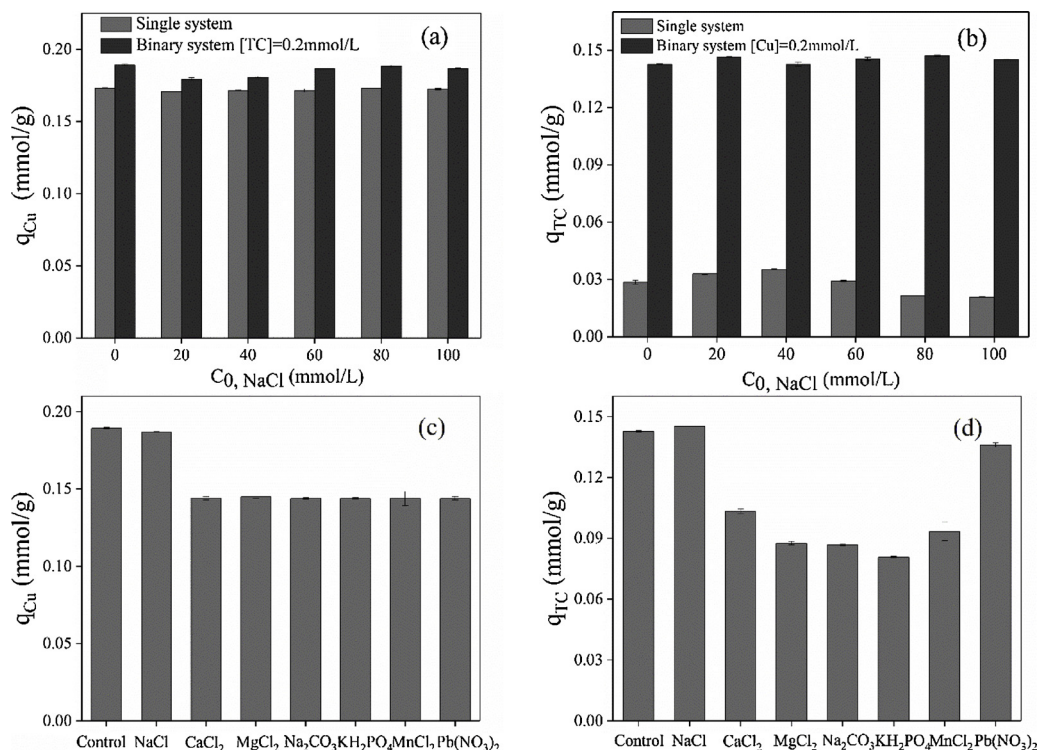
Fig. 6. Effect of ionic strength on the adsorption of Cu^{2+} (a, c) and tetracycline (TC) (b, d) in the single and binary systems (dosage = 1.0 g/L; $C_{0, Cu^{2+}}$ was fixed at 0.2 mmol/L (a, c); $C_{0, TC}$ was 0.15 mmol/L (b, d); 298 K; pH = 5).

$$\ln K^0 = \Delta S^0/R - \Delta H^0/RT \qquad (10)$$

The plot of ln K^0 versus $1/T$ should be linear with a slope equal to $\Delta H^0/R$ and an intercept equal to $\Delta S^0/R$. The calculated values of the thermodynamic parameters are listed in Table 4. As shown in Table 4, the ΔG^0 values of Cu^{2+} and TC were negative, thereby indicating that the adsorption of Cu^{2+} and TC on the SBC was a spontaneous and thermodynamically feasible process (Yu et al., 2011). With the increase in temperature, the absolute values of ΔG^0 increased. The adsorption process was more favorable at higher temperatures. Furthermore, the values of ΔH^0 for Cu^{2+} and TC were positive. The adsorption process for Cu^{2+} and TC was an endothermic reaction (Zhu et al., 2014). The ΔH^0 values for both Cu^{2+} and TC were greater than 20 kJ/mol, thereby indicating a chemisorption process. On the other hand, the positive values of ΔS^0 indicated that the adsorption process was irreversible and favorable for the sorption stability (Zhu et al., 2014).

3.7. Removal mechanism

The adsorption kinetics (Fig. S1) showed that a pseudo-second-order equation could better fit the experimental data of TC, thereby suggesting that chemisorption was involved in the process and may have been the rate-limiting step in the process of TC adsorption by SBC. Hydrogen bonding, electrostatic interaction, and π-π electron donor-

acceptor interactions may have played significant roles in the removal process of TC (Zhou et al., 2017b; Kah et al., 2017). After steam activation, the graphitic carbon ratio of BC increased. This was beneficial to the removal of TC because the graphite-like structure could act as a π-acceptor and interact with the protonated aniline ring of the TC molecule. In addition, owing to the increase in the ratio of O−C=O, the hydrogen bonding between TC and O−C=O of the SBC may have been improved. Moreover, the influence of pH on TC adsorption suggested that electrostatic interaction was involved in the removal of TC. According to the XPS results of the SBC before and after the adsorption of Cu^{2+} (Fig. 7), surface complexation between Cu^{2+} and oxygen-containing functional groups may have participated in the removal of Cu^{2+}. After Cu^{2+} uptake, the ratio of metal oxide increased from 13.71% to 18.28%, while that of the C−OH group decreased from 31.81% to 27.78%, which indirectly proved that Cu^{2+} was adsorbed on the SBC by surface complexation. Furthermore, the SBC contained ash, so precipitation or cation exchange have also been involved in the removal of Cu^{2+} (Wang et al., 2018). The impact of pH on the Cu^{2+} removal also suggested that electrostatic interaction was involved in the removal of Cu^{2+}.

According to the results of the mutual effect of Cu^{2+} and TC uptake by SBC, bridge enhancement may have participated in the synergistic adsorption process. To further confirm the bridge enhancement, XPS was applied to characterize the SBC before and after adsorption. The XPS spectrum of O1s (Fig. 7) was deconvoluted into four peaks with binding energies of 530.6, 531.49–531.78, 532.18–532.69 and 533.18–533.62 eV, which corresponded to metal oxide, C=O, C−OH, and C−O, respectively. After TC and Cu^{2+} uptake, the ratio of metal oxide in SBC + TC + Cu^{2+} was greater than that of SBC + Cu^{2+}, and that of C−OH decreased to 25.01%. This phenomenon suggested that TC may have acted as a bridge between Cu^{2+} and the adsorbent because of the formation of a TC-Cu^{2+} complex. This enhanced the adsorption capacity of Cu^{2+}. After Cu^{2+} adsorption, the three peaks were presented at 935.31, 942.86, and 954.88 eV (Fig. 7), which were assigned to Cu $2p_{3/2}$, Cu $2p_{1/2}$, and Cu $2p_{1/2}$, respectively (Jia et al.,
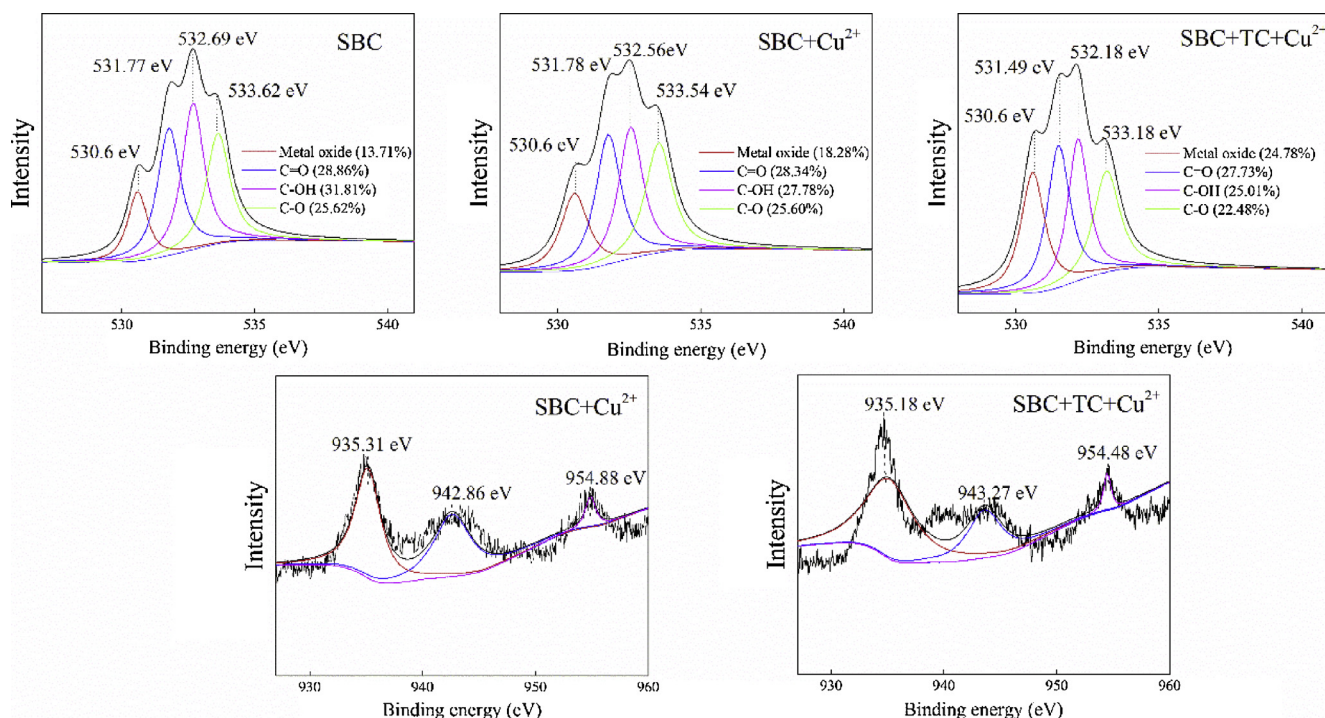
Table 4
Various thermodynamic constants for TC and Cu^{2+} adsorption onto SBC.

Target	Temperature (K)	ΔG_0 (kJ mol^{-1})	ΔH_0 (kJ mol^{-1})	ΔS_0 (J mol^{-1} K^{-1})
TC	298	−12.47	23.52	120.53
	308	−13.02		
	318	−13.95		
Cu^{2+}	298	−7.70	24.50	108.18
	308	−8.59		
	318	−9.24		

Fig. 7. X-ray photoelectron spectroscopy spectra of O1s and Cu2p in the samples of steam-activated biochar (SBC), SBC + Cu^{2+}, and SBC + tetracycline (TC) + Cu^{2+}.

2015; Wu et al., 2013). After TC adsorption, the three peaks of Cu^{2+} 2p2/3 shifted to 935.18, 943.27 and 954.48 eV, respectively, further suggesting the formation of a TC-Cu^{2+} complex (Jia et al., 2015). These results demonstrated that bridge enhancement was involved in the synergistic removal of TC and Cu^{2+}.

3.8. Potential of steam-activated biochar in actual water samples

In order to study the potential of SBC in actual water, adsorption experiments were conducted in tap water and Xiangjiang River water (the overall composition of Xiangjiang River is presented in Supporting Information). As illustrated in Table 5, SBC exhibited good adsorption performance in river and tap water. The removal efficiency of Cu^{2+} in river water was slightly higher than that of tap water and ultrapure water. This might have been attributed to the organic matter in river water, which could act as a bridge to increase the interaction between Cu^{2+} and SBC (Zhao et al., 2011). As for TC, when the Cu^{2+} concentration was 0.2 mmol/L, the removal efficiency in river water was

lower than that in tap water and ultrapure water, which might have been ascribed to the coexisting ions (Table S1). These ions may have competed for the active adsorption sites. When the Cu^{2+} concentration increased from 1.0 mmol/L to 2.0 mmol/L, the removal efficiency of TC in the river water was higher than that in ultrapure water. The increased amount of TC may have been adsorbed by complexation with the increased adsorbed Cu^{2+}. The complex acted as a bridge between Cu^{2+} and the adsorbent. When $C_{TC} = 0.2$ mmol/L and $C_{Cu^{2+}} = 2.0$ mmol/L, the adsorption efficiency of SBC for Cu^{2+} and TC reached 84.0% and 84.5% in river water, respectively. SBC showed great application potential for the simultaneous removal of TC and Cu^{2+} from actual water.

3.9. Reusability test

The reusability of SBC for the adsorption of TC and Cu^{2+} in binary systems was investigated by repeating the adsorption–desorption cycle for four times. As shown in Fig. 8, after three cycles, the removal efficiency of TC and Cu^{2+} by the SBC decreased to approximately 83.25% and 80.59%, respectively. SBC exhibited excellent reusability for the adsorption of both target compounds.

4. Conclusions

In this study, TC and Cu^{2+} could be effectively and simultaneously removed by SBC. When $C_{TC} = 0.15$ mmol/L and $C_{Cu} = 0.20$ mmol/L, the removal efficiency of TC and Cu^{2+} reached 95.75% and 94.66%, respectively. Bridge enhancement and site competition were involved in the synergistic adsorption of TC and Cu^{2+}. SBC exhibited good adsorption capacity for TC and Cu^{2+} in tap water and river water. SBC is a promising adsorbent for the removal of combined pollution containing TC and Cu^{2+}. This work provided an effective method for the simultaneous removal of antibiotics and heavy metals from aquatic environments.
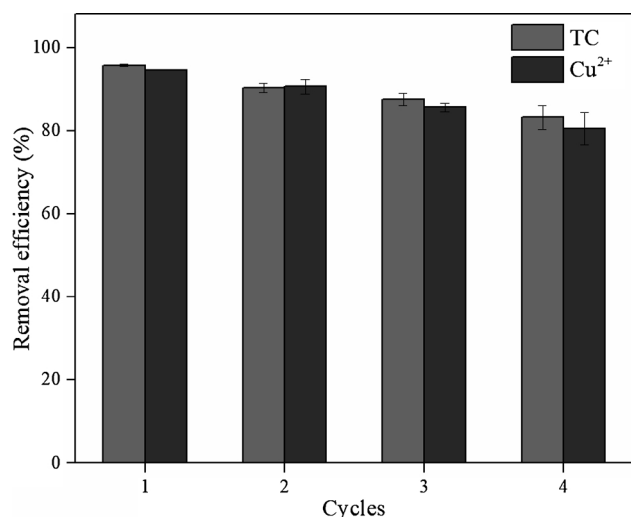
Table 5
Practical application of SBC in Co-removal of Cu^{2+} and TC in different waters.

Solutions (mmol/L)	Water[a]	$C_{e,TC}$[b]	$A_{e,TC}$[c]	$C_{e,Cu^{2+}}$[b]	$A_{e,Cu^{2+}}$[c]
$C_{0,Cu^{2+}} = 0.2$, $C_{0,TC} = 0.2$	UW	0.132	66.0	0.185	92.5
	TW	0.115	57.5	0.186	93.0
	RW	0.107	53.5	0.188	94.0
$C_{0,Cu^{2+}} = 1.0$, $C_{0,TC} = 0.2$	UW	0.138	69.0	0.862	86.2
	TW	0.177	88.5	0.874	87.4
	RW	0.147	73.5	0.882	88.2
$C_{0,Cu^{2+}} = 2.0$, $C_{0,TC} = 0.2$	UW	0.140	70.0	1.619	81.0
	TW	0.187	93.5	1.666	83.3
	RW	0.169	84.5	1.680	84.0

[a] UW, TW, and RW are ultrapure water, tap water, and river water, respectively.

[b] $C_{e,TC}$ and $C_{e,Cu}$ are the adsorption capacity of TC and Cu^{2+}, respectively.

[c] $A_{e,TC}$ and $A_{e,Cu}$ are the removal efficiency of TC and Cu, respectively. The units of C_e and A are mmol/g and %, respectively. The pH of UW, TW, and RW are 7.04, 6.91 and 7.15, respectively.

Fig. 8. Reusability test of steam-activated biochar for the adsorption of tetracycline (TC) and Cu^{2+} (dosage = 1.0 g/L; $C_{0, Cu^{2+}}$ was fixed at 0.2 mmol/L; $C_{0, TC}$ was 0.15 mmol/L; 298 K; pH = 5).

Declaration of Competing Interest

None.

Acknowledgements

Appendix A. Supplementary data

Supplementary material related to this article can be found, in the online version, at doi:https://doi.org/10.1016/j.jhazmat.2019.121470.

References

Azargohar, R., Dalai, A.K., 2008. Steam and KOH activation of biochar: experimental and modeling studies. Microporous Mesoporous Mater. 110, 413–421. https://doi.org/10.1016/j.micromeso.2007.06.047.

Baig, S.A., Jin, Z., Muhammad, N., Sheng, T., Xu, X., 2014. Effect of synthesis methods on magnetic Kans grass biochar for enhanced As(III, V) adsorption from aqueous solutions. Biomass Bioenergy 71, 299–310. https://doi.org/10.1016/j.biombioe.2014.09.027.

Chen, A., Shang, C., Shao, J., Lin, Y., Luo, S., Zhang, J., Huang, H., Lei, M., Zeng, Q., 2016. Carbon disulfide-modified magnetic ion-imprinted chitosan-Fe(III): a novel adsorbent for simultaneous removal of tetracycline and cadmium. Carbohydr. Polym. 155, 19–27. https://doi.org/10.1016/j.carbpol.2016.08.038.

Dehghan, A., Zarei, A., Jaafari, J., Shams, M., Mousavi, K.A., 2018. Tetracycline removal from aqueous solutions using zeolitic imidazolate frameworks with different morphologies: a mathematical modeling. Chemosphere 217, 250–260. https://doi.org/10.1016/j.chemosphere.2018.10.166.

Dehghani, M.H., Zarei, A., Mesdaghinia, A., Nabizadeh, R., Alimohammadi, M., Afsharnia, M., 2017a. Adsorption of Cr (VI) ions from aqueous systems using thermally sodium organo-bentonite biopolymer composite (TSOBC): response surface methodology, isotherm, kinetic and thermodynamic studies. Desalin. Water Treat. 85, 298–312. https://doi.org/10.5004/dwt.2017.21306.

Dehghani, M.H., Zarei, A., Mesdaghinia, A., Nabizadeh, R., Alimohammadi, M., Afsharnia, M., 2017b. Response surface modeling, isotherm, thermodynamic and optimization study of arsenic (V) removal from aqueous solutions using modified bentonite-chitosan (MBC). Korean J. Chem. Eng. 34, 757–767. https://doi.org/10.1007/s11814-016-0330-0.

Dehghani, M.H., Tajik, S., Panahi, A., Khezri, M., Zarei, A., Heidarinejad, Z., Yousefi, M.,

2018. Adsorptive removal of noxious cadmium from aqueous solutions using poly urea-formaldehyde: a novel polymer adsorbent. MethodsX 5, 1148–1155. https://doi.org/10.1016/j.mex.2018.09.010.

Ding, J., Li, Q., Xu, X., Zhang, X., Su, Y., Yue, Q., Gao, B., 2018. A wheat straw cellulose-based hydrogel for Cu (II) removal and preparation copper nanocomposite for reductive degradation of chloramphenicol. Carbohydr. Polym. 190, 12–22. https://doi.org/10.1016/j.carbpol.2018.02.032.

Fazlzadeh, M., Rahmani, K., Zarei, A., Abdoallahzadeh, H., Nasiri, F., Khosravi, R., 2017a. A novel green synthesis of zero valent iron nanoparticles (NZVI) using three plant extracts and their efficient application for removal of Cr(VI) from aqueous solutions. Adv. Powder Technol. 28, 122–130. https://doi.org/10.1016/j.apt.2016.09.003.

Fazlzadeh, M., Khosravi, R., Zarei, A., 2017b. Green synthesis of zinc oxide nanoparticles using Peganum harmala seed extract, and loaded on Peganum harmala seed powdered activated carbon as new adsorbent for removal of Cr(VI) from aqueous solution. Ecol. Eng. 103, 180–190. https://doi.org/10.1016/j.ecoleng.2017.02.052.

Gong, X., Huang, D., Liu, Y., Zeng, G., Wang, R., Wan, J., Zhang, C., Cheng, M., Qin, X., Xue, W., 2017. Stabilized nanoscale zero-valent iron mediated cadmium accumulation and oxidative damage of Boehmeria nivea (L.) Gaudich cultivated in cadmium contaminated sediments. Environ. Sci. Technol. 51. https://doi.org/10.1021/acs.est.7b03164.

Gong, X., Huang, D., Liu, Y., Zeng, G., Wang, R., Wei, J., Huang, C., Xu, P., Wan, J., Zhang, C., 2018. Pyrolysis and reutilization of plant residues after phytoremediation of heavy metals contaminated sediments: for heavy metals stabilization and dye adsorption. Bioresour. Technol. 253, 64–71. https://doi.org/10.1016/j.biortech.2018.01.018.

Gong, X., Huang, D., Liu, Y., Zeng, G., Chen, S., Wang, R., Xu, P., Cheng, M., Zhang, C., Xue, W., 2019. Biochar facilitated the phytoremediation of cadmium contaminated sediments: metal behavior, plant toxicity, and microbial activity. Sci. Total Environ. 666, 1126–1133. https://doi.org/10.1016/j.scitotenv.2019.02.215.

Guo, X., Peng, Z., Huang, D., Xu, P., Zeng, G., Zhou, S., Gong, X., Cheng, M., Deng, R., Yi, H., Luo, H., Yan, X., Li, T., 2018. Biotransformation of cadmium-sulfamethazine combined pollutant in aqueous environments: phanerochaete chrysosporium bring cautious optimism. Chem. Eng. J. 347, 74–83. https://doi.org/10.1016/j.cej.2018.04.089.

Hong, X., Fang, C., Hui, K.S., Hui, K.N., Zhuang, H., Liu, W., Shan, S., 2017. Influence of interfering anions on Cu^{2+} and Zn^{2+} ions removal on chestnut outer shell-derived hydrochars in aqueous solution. RSC Adv. 7, 51199–51205. https://doi.org/10.1039/c7ra10384k.

Huang, H., Zou, Y.L., Li, Y.N., 2012. Experimental and modeling studies of sorption of tetracycline onto zeolite in the presence of copper(II). Adv. Mater. Res. 512–515, 2355–2360. https://doi.org/10.4028/www.scientific.net/AMR.512-515.2355.

Huang, D.L., Wang, R.Z., Liu, Y.G., Zeng, G.M., Lai, C., Xu, P., Lu, B.A., Xu, J.J., Wang, C., Huang, C., 2015. Application of molecularly imprinted polymers in wastewater treatment: a review. Environ. Sci. Pollut. Res. 22, 963–977. https://doi.org/10.1007/s11356-014-3599-8.

Huang, D., Hu, C., Zeng, G., Cheng, M., Xu, P., Gong, X., Wang, R., Xue, W., 2016. Combination of Fenton processes and biotreatment for wastewater treatment and soil remediation. Sci. Total Environ. 574, 1599–1610. https://doi.org/10.1016/j.scitotenv.2016.08.199.

Huang, D., Tang, Z., Peng, Z., Lai, C., Zeng, G., Zhang, C., Xu, P., Cheng, M., Wan, J., Wang, R., 2017. Fabrication of water-compatible molecularly imprinted polymer based on β-cyclodextrin modified magnetic chitosan and its application for selective removal of bisphenol A from aqueous solution. J. Taiwan Inst. Chem. Eng. 77, 113–121. https://doi.org/10.1016/j.jtice.2017.04.030.

Huang, D., Deng, R., Wan, J., Zeng, G., Xue, W., Zhou, C., Hu, L., Liu, X., Xu, P., Guo, X., Ren, X., 2018. Remediation of lead-contaminated sediment by biochar-supported nano-chlorapatite: Accompanied with the change of available phosphorus and organic matters. J. Hazard. Mater. 348, 109–116. https://doi.org/10.1016/j.jhazmat.2018.01.024.

Huang, D., Luo, H., Zhang, C., Zeng, G., Lai, C., Chen, M., Wang, R., Deng, R., Xue, W., Gong, X., Guo, X., Li, T., 2019a. Nonnegligible role of biomass types and its compositions on the formation of persistent free radicals in biochar: insight into the influences on Fenton-like process. Chem. Eng. J. 361, 353–363. https://doi.org/10.1016/j.cej.2018.12.098.

Huang, D., Liu, C., Zhang, C., Deng, R., Wang, R., Xue, W., Luo, H., Zeng, G., Zhang, Q., Guo, X., 2019b. Cr(VI) removal from aqueous solution using biochar modified with Mg/Al-layered double hydroxide intercalated with ethylenediaminetetraacetic acid. Bioresour. Technol. 276, 127–132. https://doi.org/10.1016/j.biortech.2018.12.114.

Jia, S., Yang, Z., Yang, W., Zhang, T., Zhang, S., Yang, X., Dong, Y., Wu, J., Wang, Y., 2015. Removal of Cu(II) and tetracycline using an aromatic rings-functionalized chitosan-based flocculant: enhanced interaction between the flocculant and the antibiotic. Chem. Eng. J. 283, 495–503. https://doi.org/10.1016/j.cej.2015.08.003.

Jin, K., Liu, H., Zheng, Y.M., Qu, J., Chen, J.P., 2010. Systematic study of synergistic and antagonistic effects on adsorption of tetracycline and copper onto a chitosan. J. Colloid Interface Sci. 344, 117–125. https://doi.org/10.1016/j.jcis.2009.11.049.

Jung, K.W., Lee, S.Y., Lee, Y.J., 2018. Hydrothermal synthesis of hierarchically structured birnessite-type MnO_2/biochar composites for the adsorptive removal of Cu(II) from aqueous media. Bioresour. Technol. 204–212. https://doi.org/10.1016/j.biortech.2018.03.125.

Kah, M., Sigmund, G., Xiao, F., Hofmann, T., 2017. Sorption of ionizable and ionic organic compounds to biochar, activated carbon and other carbonaceous materials. Water Res. 124, 673–692. https://doi.org/10.1016/j.watres.2017.07.070.

Khosravi, R., Eslami, H., Zarei, A., Heidari, M., Baghani, A.N., Safavi, N., Mokammel, A., Fazlzadeh, M., Adhami, S., 2018a. Comparative evaluation of nitrate adsorption from aqueous solutions using green and red local montmorillonite adsorbents. Desalin. Water Treat. 116, 119–128. https://doi.org/10.5004/dwt.2018.22577.

Khosravi, R., Zarei, A., Heidari, M., Ahmadfazeli, A., Vosughi, M., Fazlzadeh, M., 2018b. Application of ZnO and TiO$_2$ nanoparticles coated onto montmorillonite in the presence of H$_2$O$_2$ for efficient removal of cephalexin from aqueous solutions. Korean J. Chem. Eng. 35, 1000–1008. https://doi.org/10.1007/s11814-018-0005-0.

Lai, C., Wang, M.M., Zeng, G.M., Liu, Y.G., Huang, D.L., Zhang, C., Wang, R.Z., Xu, P., Cheng, M., Huang, C., 2016. Synthesis of surface molecular imprinted TiO 2 /graphene photocatalyst and its highly efficient photocatalytic degradation of target pollutant under visible light irradiation. Appl. Surf. Sci. 390, 368–376. https://doi.org/10.1016/j.apsusc.2016.08.119.

Ling, C., Liu, F.Q., Xu, C., Chen, T.P., Li, A.M., 2013. An integrative technique based on synergistic coremoval and sequential recovery of copper and tetracycline with dual-functional chelating resin: roles of amine and carboxyl groups. ACS Appl. Mater. Interface 5, 11808–11817. https://doi.org/10.1021/am403491b.

Ma, Y., Zhou, Q., Zhou, S., Wang, W., Jin, J., Xie, J., Li, A., Shuang, C., 2014. A bifunctional adsorbent with high surface area and cation exchange property for synergistic removal of tetracycline and Cu^{2+}. Chem. Eng. J. 258, 26–33. https://doi.org/10.1016/j.cej.2014.07.096.

Mandal, S., Sarkar, B., Igalavithana, A.D., Ok, Y.S., Yang, X., Lombi, E., Bolan, N., 2017. Mechanistic insights of 2,4-D sorption onto biochar: influence of feedstock materials and biochar properties. Bioresour. Technol. 246, 160–167. https://doi.org/10.1016/j.biortech.2017.07.073.

Naghizadeh, A., Shahabi, H., Ghasemi, F., Zarei, A., 2016. Synthesis of walnut shell modified with titanium dioxide and zinc oxide nanoparticles for efficient removal of humic acid from aqueous solutions. J. Water Health 14, 989–997. https://doi.org/10.2166/wh.2016.072.

Qasemi, M., Afsharnia, M., Farhang, M., Bakhshizadeh, A., Allahdadi, M., Zarei, A., 2018a. Health risk assessment of nitrate exposure in groundwater of rural areas of Gonabad and Bajestan, Iran. Environ. Earth Sci. 77, 551. https://doi.org/10.1007/s12665-018-7732-8.

Qasemi, M., Farhang, M., Biglari, H., Afsharnia, M., Ojrati, A., Khani, F., Samiee, M., Zarei, A., 2018b. Health risk assessments due to nitrate levels in drinking water in villages of Azadshahr, northeastern Iran. Environ. Earth Sci. 77, 782. https://doi.org/10.1007/s12665-018-7973-6.

Qasemi, M., Zarei, A., Afsharnia, M., Salehi, R., Allahdadi, M., Farhang, M., 2018c. Data on cadmium removal from synthetic aqueous solution using garbage ash. Data Brief 20, 1115–1123. https://doi.org/10.1016/j.dib.2018.08.163.

Qasemi, M., Afsharnia, M., Zarei, A., Najafpoor, A., Salari, S., Shams, M., 2018d. Phenol removal from aqueous solution using Citrullus colocynthis waste ash. Data Brief 18, 620–628. https://doi.org/10.1016/j.dib.2018.03.049.

Qasemi, M., Shams, M., Sajjadi, S.A., Farhang, M., Erfanpoor, S., Yousefi, M., Zarei, A., Afsharnia, M., 2019. Cadmium in groundwater consumed in the rural areas of Gonabad and Bajestan, Iran: occurrence and health risk assessment. Biol. Trace Elem. Res. 1–10. https://doi.org/10.1007/s12011-019-1660-7.

Rajapaksha, A.U., Vithanage, M., Zhang, M., Ahmad, M., Mohan, D., Chang, S.X., Ok, Y.S., 2014. Pyrolysis condition affected sulfamethazine sorption by tea waste biochars. Bioresour. Technol. 166, 303–308. https://doi.org/10.1016/j.biortech.2014.05.029.

Rajapaksha, A.U., Vithanage, M., Ahmad, M., Seo, D.C., Cho, J.S., Lee, S.E., Lee, S.S., Ok, Y.S., 2015. Enhanced sulfamethazine removal by steam-activated invasive plant-derived biochar. J. Hazard. Mater. 290, 43–50. https://doi.org/10.1016/j.jhazmat.2015.02.046.

Rajapaksha, A.U., Vithanage, M., Sang, S.L., Seo, D.C., Tsang, D.C.W., Yong, S.O., 2016. Steam activation of biochars facilitates kinetics and pH-resilience of sulfamethazine sorption. J. Soils Sediment. 16, 889–895. https://doi.org/10.1007/s11368-015-1325-x.

Rezaei, H., Zarei, A., Kamarehie, B., Jafari, A., Fakhri, Y., Bidarpoor, F., Karami, M.A., Farhang, M., Ghaderpoori, M., Sadeghi, H., 2019. Levels, Distributions and Health Risk Assessment of Lead, Cadmium and Arsenic Found in Drinking Groundwater of Dehgolan's Villages, Iran. Toxicol. Environ. Health Sci. 11, 54–62. https://doi.org/10.1007/s13530-019-0388-2.

Sarmah, A.K., Meyer, M.T., Boxall, A.B., 2006. A global perspective on the use, sales, exposure pathways, occurrence, fate and effects of veterinary antibiotics (VAs) in the environment. Chemosphere 65, 725–759. https://doi.org/10.1016/j.chemosphere.2006.03.026.

Shim, T., Yoo, J., Ryu, C., Park, Y.K., Jung, J., 2015. Effect of steam activation of biochar produced from a giant Miscanthus on copper sorption and toxicity. Bioresour. Technol. 197, 85–90. https://doi.org/10.1016/j.biortech.2015.08.055.

Wang, H., Gao, B., Wang, S., Fang, J., Xue, Y., Yang, K., 2015. Removal of Pb(II), Cu(II), and Cd(II) from aqueous solutions by biochar derived from KMnO$_4$ treated hickory wood. Bioresour. Technol. 197, 356–362. https://doi.org/10.1016/j.biortech.2015.08.132.

Wang, R.Z., Huang, D.L., Liu, Y.G., Zhang, C., Lai, C., Zeng, G.M., Cheng, M., Gong, X.M., Wan, J., Luo, H., 2018. Investigating the adsorption behavior and the relative distribution of Cd^{2+} sorption mechanisms on biochars by different feedstock. Bioresour. Technol. 261, 265–271.

Wang, Y., Wang, X., Li, J., Li, Y., Xia, S., Zhao, J., Minale, T.M., Gu, Z., 2019. Coadsorption of tetracycline and copper(II) onto struvite loaded zeolite – an environmentally friendly product recovered from swine biogas slurry. Chem. Eng. J. 371, 366–377. https://doi.org/10.1016/j.cej.2019.04.058.

Wu, L., Wang, H., Lan, H., Liu, H., Qu, J., 2013. Adsorption of Cu(II)–EDTA chelates on tri-ammonium-functionalized mesoporous silica from aqueous solution. Sep. Purif. Technol. 117, 118–123. https://doi.org/10.1016/j.seppur.2013.06.016.

Yap, M.W., Mubarak, N.M., Sahu, J.N., Abdullah, E.C., 2016. Microwave induced synthesis of magnetic biochar from agricultural biomass for removal of lead and cadmium from wastewater. J. Ind. Eng. Chem. 287–295. https://doi.org/10.1016/j.jiec.2016.09.036.

Yu, X.Y., Luo, T., Zhang, Y.X., Jia, Y., Zhu, B.J., Fu, X.C., Liu, J.H., Huang, X.J., 2011. Adsorption of lead(II) on O$_2$-plasma-oxidized multiwalled carbon nanotubes: thermodynamics, kinetics, and desorption. ACS Appl. Mater Interface 3, 2585–2593. https://doi.org/10.1021/am2004202.

Yu, Q., Deng, S., Yu, G., 2017. Selective removal of perfluorooctane sulfonate from aqueous solution using chitosan-based molecularly imprinted polymer adsorbents. Water Res. 124, 673–692. https://doi.org/10.1016/j.watres.2017.07.070.

Zeng, Z.W., Tian, S.R., Liu, Y.G., Tan, X.F., Zeng, G.M., Jiang, L.H., Yin, Z.H., Liu, N., Liu, S.B., Li, J., 2017. Comparative study of rice husk biochars for aqueous antibiotics removal: biochars application for aqueous antibiotics removal. J. Chem. Technol. Biotechnol. 93, 1075–1084. https://doi.org/10.1002/jctb.5464.

Zhang, Z., Liu, H., Wu, L., Lan, H., Qu, J., 2015. Preparation of amino-Fe(III) functionalized mesoporous silica for synergistic adsorption of tetracycline and copper. Chemosphere 138, 625–632. https://doi.org/10.1016/j.chemosphere.2015.07.014.

Zhao, Y., Geng, J., Wang, X., Gu, X., Gao, S., 2011. Adsorption of tetracycline onto goethite in the presence of metal cations and humic substances. J. Colloid Interface Sci. 361, 247–251. https://doi.org/10.1016/j.jcis.2011.05.051.

Zhao, Y., Tan, Y., Guo, Y., Gu, X., Wang, X., Zhang, Y., 2013. Interactions of tetracycline with Cd (II), Cu (II) and Pb (II) and their cosorption behavior in soils. Environ. Pollut. 180, 206–213. https://doi.org/10.1016/j.envpol.2013.05.043.

Zhou, L., Liu, Y., Liu, S., Yin, Y., Zeng, G., Tan, X., Hu, X., Hu, X., Jiang, L., Ding, Y., 2016. Investigation of the adsorption-reduction mechanisms of hexavalent chromium by ramie biochars of different pyrolytic temperatures. Bioresour. Technol. 218, 351–359. https://doi.org/10.1016/j.biortech.2016.06.102.

Zhou, C., Lai, C., Huang, D., Zeng, G., Zhang, C., Cheng, M., Hu, L., Wan, J., Xiong, W., Wen, M., 2017a. Highly porous carbon nitride by supramolecular preassembly of monomers for photocatalytic removal of sulfamethazine under visible light driven. Appl. Catal. B Environ. 220, 202–210. https://doi.org/10.1016/j.apcatb.2017.08.055.

Zhou, Y., Liu, X., Xiang, Y., Wang, P., Zhang, J., Zhang, F., Wei, J., Luo, L., Lei, M., Tang, L., 2017b. Modification of biochar derived from sawdust and its application in removal of tetracycline and copper from aqueous solution: adsorption mechanism and modelling. Bioresour. Technol. 245, 266–273. https://doi.org/10.1016/j.biortech.2017.08.178.

Zhou, X., Lai, C., Huang, D., Zeng, G., Chen, L., Qin, L., Xu, P., Cheng, M., Huang, C., Zhang, C., 2018. Preparation of water-compatible molecularly imprinted thiol-functionalized activated titanium dioxide: selective adsorption and efficient photo-degradation of 2, 4-dinitrophenol in aqueous solution. J. Hazard. Mater. 346, 113–123. https://doi.org/10.1016/j.jhazmat.2017.12.032.

Zhu, X., Liu, Y., Feng, Q., Chao, Z., Zhang, S., Chen, J., 2014. Preparation of magnetic porous carbon from waste hydrochar by simultaneous activation and magnetization for tetracycline removal. Bioresour. Technol. 154, 209–214. https://doi.org/10.1016/j.biortech.2013.12.019.